A STUDY OF RC MEMBERS STRENGTHENED WITH A LONGITUDINALLY PRESTRESSED CONCRETE JACKET

(Translation from Proceedings of JSCE, No. 683/V-52, 1-12, Aug. 2001)

Takashi YAMAMOTO Atsushi HATTORI Toyo MIYAGAWA

In seismic strengthening with a reinforced concrete jacket, the application of longitudinal prestress to the jacketing concrete is one means of controlling crack propagation and improving elastic restoration behavior. In this study, the influence of longitudinal prestress, mechanical properties of the tendons, and confinement ratio on crack propagation, failure mode, ductility, and elastic restoration behavior are investigated under load reversal. The results indicate that longitudinal prestress effectively controls crack propagation and improves elastic restoration behavior if high strength and high elastic modulus tendons are used. Furthermore, it is demonstrated that elastic restoration behavior is related to the ductility of the strengthened member in the post-peak region.

Key Words: *strengthening, reinforced concrete jacketing, longitudinal prestress, elastic restoration, ductility, mechanical properties of tendons, confinement ratio*

Takashi Yamamoto is a Research Associate in the Department of Civil Engineering at Kyoto University, Kyoto, Japan. He obtained his Dr. Eng. from Kyoto University in 2001. His research interests relate to performance in strengthened reinforced concrete member. He is a member of JSMS, JCI, and JSCE.

Atsushi Hattori is an Associate Professor in the Department of Civil Engineering at Kyoto University, Kyoto, Japan. He obtained his Dr. Eng. from Kyoto University in 2000. His research interests include application of fiber-reinforced materials to concrete structures and structural durability. He is a member of JSMS, JCI, and JSCE

Toyo Miyagawa is a Professor in the Department of Civil Engineering, Kyoto University, Kyoto, Japan. He received his Dr. Eng. from Kyoto University in 1985. He is the author of a number of papers dealing with durability, maintenance, repair, and scenario design of reinforced concrete structures. He is a member of ACI, RILEM, fib, JSMS, JCI, and JSCE.

1. INTRODUCTION

A large number of concrete piers were damaged in the Hyogoken-Nanbu earthquake due to insufficient flexural capacity, shear capacity, or ductility. Further, some concrete piers have had to be removed or reconstructed, since large residual deformations rendered the bridges unsuitable for continued use after the earthquake [1]. Since the earthquake, seismic strengthening of existing concrete bridge piers has been in progress so as to improve their flexural capacity, shear capacity, and/or ductility. The application of longitudinal prestressing to RC members being strengthened using a reinforced concrete jacket may provide the desired improvements. Since this method also controls crack propagation and improves elastic restoration behavior, it should also be advantageous as regards rapid restoration of bridges to serviceability after an earthquake.

To protect RC piers during earthquake, when large horizontal loading is possible, it is necessary (through seismic or seismic strengthening design) to provide adequate ductility to absorb the energy imparted by the load. However, an RC member strengthened in this way may suffer brittle failure, which is early compression failure or rupture of the tendons due to prestressing.

The objective of this study is to investigate the flexural behavior, from the viewpoints of ductility and elastic restoration behavior, of an RC member strengthened with a longitudinally prestressed concrete jacket under reversed cyclic loading. The results are compared with the behavior of an un-strengthened member, one strengthened using carbon fiber sheeting, and one strengthened with an RC jacket. The following test parameters are considered: amount of longitudinal prestress, mechanical properties of the prestressing tendons, and confinement ratio in the compression zone of the strengthened member. Furthermore, the distribution and degree of longitudinal prestress and the flexural behavior of a member strengthened with a longitudinally prestressed concrete jacket are simulated using two-dimensional finite element analysis with discrete elements, such as bond linkage elements to represent bonding between existing and jacketing concrete.

2. EXPERIMENTAL OUTLINE

Although the ultimate aim was to investigate the behavior of columns, on which flexural, shear and axial load worked, the loading test using beam type specimens (which include no influence of shear force in the flexural span) was adopted as a way to investigate the fundamental flexural behavior of a strengthened member.

Table 1 Mechanical properties of longitudinal reinforcement or tendon

	Yield strength (N/mm^2)	Tensile strength (N/mm^2)	Young's modulus (N/mm^2)	Ultimate strain (%)
SD295A D13	356	517	210000	26.8
CF sheet[2)]	—	3479	230300	1.5[1)]
SBPRϕ11	1347	1410	199900	9.0
CFRPϕ11	—	2100	156800	1.3[1)]
AFRPϕ11	—	1493	68600	2.2[1)]

1) Ultimate strain = Tensile strength/ Young's modulus
2) Sheet width: 250mm, $200g/m^2$

2.1 Experimental parameters

a) Longitudinal prestress

The basic tensile force applied to one steel tendon (SBPR930/1080 ϕ11mm) was 53.0 kN, giving a ratio to yield strength (P_r) of 0.60 as determined by the limit tensile stress immediately after introducing tension, which was $0.70f_{puk}(0.85f_{pyk})$ [2]. Further, In order to investigate the influence of degree of longitudinal prestress, P_r=0.00 (0.0 kN) and P_r=0.30 (26.5 kN) were also tested. In the case of the carbon/aramid fiber reinforced plastic rod (CFRP or AFRP) tendons, the tension values were 26.5 kN and 53.0 kN. These values correspond to P_r=0.15 and P_r=0.30 for the ϕ11 mm CFRP tendon and P_r=0.21 and P_r=0.42 for the ϕ11 mm AFRP tendon, respectively. The longitudinal prestress was the compression of the jacketing concrete as measured at the center of depth of the mid-span in a strengthened specimen.

b) Mechanical properties of longitudinal reinforcement

In order to investigate the influence of the mechanical properties of the longitudinal reinforcement, tests were carried out with deformed reinforcing steel (SD295A-D13), a steel tendon (SBPR930/1080 ϕ11mm), CFRP(ϕ11mm), and AFRP(ϕ11mm). A specimen strengthened longitudinally with carbon fiber sheeting was also prepared. The mechanical properties of the various longitudinal reinforcements are given in Table 1.

c) Volumetric confinement ratio

When a specimen is strengthened with a reinforcing jacket, the volumetric confinement ratio represents the

degree of confinement in the compression zone of the jacketing concrete. It was determined by limitation of lateral reinforcement [2] and by effective value for improvement of ductility. The selected volumetric confinement ratios were ρ_v=0.92%, 0.69%, and 0.46%. These ratios corresponded to lateral reinforcement spacings of s=44mm, 59mm, and 88mm, respectively.

2.2 Specimens

a) Specimen without strengthening (control specimen)
Details of the reinforced concrete control specimen (without strengthening) are given in Fig. 1. The control specimen measured 200 x 200 mm in cross section, and had a span of 1,800 mm with 8 x SD295A D16 reinforcing steel rods. Based on the minimum reinforcement specified in [3], transverse hoop reinforcement (SD295A D6) were provided at a spacing of 200 mm in the longitudinal direction. The ratio of shear capacity to flexural capacity was 1.15. A compressive normal force of 108 kN was applied by means of an unbonded tendon (SBPR930/1080 ϕ17 mm) located at the center of the section. The objective concrete compressive strength was 27 N/mm^2.

b) Specimen strengthened with reinforced concrete jacket
Details of the jacket-strengthened specimens using reinforced concrete or longitudinally prestressed concrete are shown in Fig. 2. The strengthened specimens had a 300 x 300 mm cross section and a span of 1,800 mm. The jacket concrete thickness was 50 mm. Although, strengthening with a reinforced concrete jacket would in practice involve jacketing concrete of approximately 30 mm over an existing cross section of 200 x 200mm, the somewhat greater thickness of 50 mm was adopted here so as to prevent failure at the anchorage during the prestressing operation. The spacing of the transverse reinforcement in the shear zone was 100 mm. Shear reinforcement in the horizontal section with D6 hoops or FRP spirals resulted in shear reinforcement ratios of 0.21% and 0.14%, respectively. In order to ensure bonding between the existing concrete and the new jacket, the new concrete was cast after roughening the surface layer of the existing concrete with a retarder.

The longitudinal forces described in 2.1 a) above were imposed on only the jacket concrete section by applying a square cut-out plate to the edge of the specimen. However, the prestress was transmitted to the existing portion through the bond between existing concrete and new. Although un-bonded tendons are less likely to rupture in the flexural ultimate state during post-tensioning than bonded tendons, the bonded type were selected in order to avoid problems of tendon corrosion resulting from the tendon's position close to the extreme edge of the cross-section.

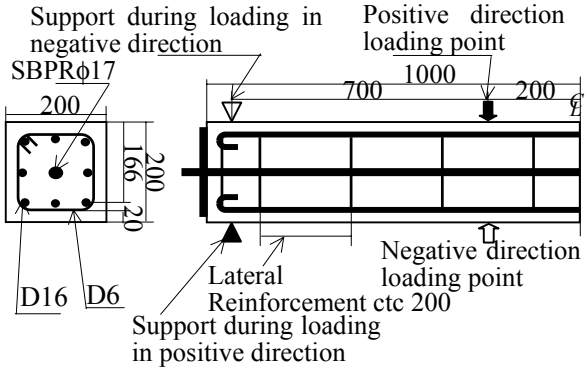

Fig.1 Details of unstrengthened specimen (unit: mm)

The following procedure was used to prepare specimens strengthened with longitudinally prestressed concrete:

1. Casting and curing of existing concrete
2. Introduction of normal force, such as an axial force ratio of 10%
3. Installation of reinforcement for the jacketing portion around the existing specimen
4. Casting and curing of jacketing concrete
5. Introduction of longitudinal prestress, adjustment of normal force, and injection of grout

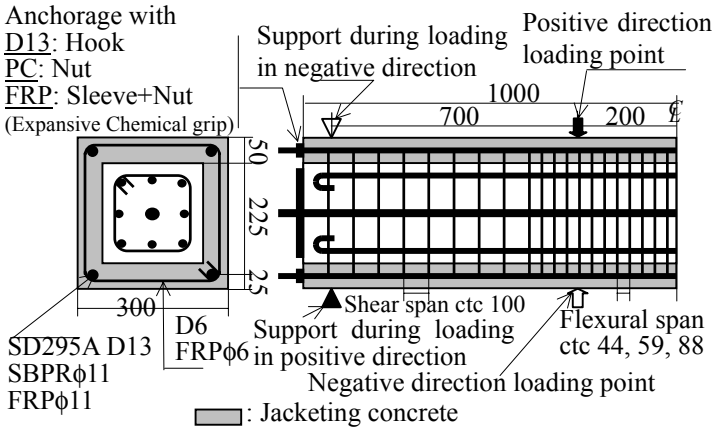

Fig.2 Details of strengthened specimen (unit: mm)

Table 2 Experimental parameters and specimens

Specimen	Axial force ratio (%)	Existing	Jacketing (Volumetric confinement ratio: in flexural span)				Longitudinal prestress	
		f'_c N/mm^2	Longitudinal	Lateral	Volumetric confinement ratio ρ_v(%)	f'_c N/mm^2	Tension (kN)	Prestress (N/mm^2)
Control	12.6	45.9	—	—	—	—	—	—
CS	12.1	44.8	CF sheet	CF sheet	0.28	—	—	—
RC1-0	9.7	40.3	SD295A D13	SD295A D6 stirrup	0.92	50.0	—	—
RC3-0	9.3	40.3	SD295A D13	SD295A D6 stirrup	0.46	50.0	—	—
PC1-0	10.5	33.1	SBPR ϕ11	SD295A D6 stirrup	0.92	45.9	0.0	0.00
PC1-1	10.7	33.1	SBPR ϕ11	SD295A D6 stirrup	0.92	45.9	26.5	1.03
PC1-2	11.5	45.1	SBPR ϕ11	SD295A D6 stirrup	0.92	45.4	53.0	2.60
PC2-2	11.6	45.1	SBPR ϕ11	SD295A D6 stirrup	0.69	45.4	53.0	1.36
PC3-2	10.6	40.2	SBPR ϕ11	SD295A D6 stirrup	0.46	40.2	53.0	2.29
CFPC1-1	10.5	35.5	CFRP ϕ11	CFRP spiral ϕ6	0.92	46.9	26.5	1.22
CFPC1-2	11.1	38.3	CFRP ϕ11	CFRP spiral ϕ6	0.92	45.5	53.0	2.83
AFPC1-1	10.9	35.5	AFRP ϕ11	AFRP spiral ϕ6	0.92	46.9	26.5	0.94
AFPC1-2	11.3	38.3	AFRP ϕ11	AFRP spiral ϕ6	0.92	45.5	53.0	3.03

c) Specimen strengthened with carbon fiber sheeting
Firstly, carbon fiber sheeting of 2.5 layers were bonded longitudinally to the existing specimen described in 2.2 a). The amount of longitudinal sheeting corresponded to the size of the tendon in a specimen strengthened with CFRP using as an index $p_f=A_f/b/d_f$), where A_f is the cross-sectional area of the CFRP sheeting or CFRP rod, b is the width of the specimen, and d_f is effective depth of the CFRP sheeting or CFRP rod. The sheeting of 2.5 layers consisted of sheets of 2 layers with 200mm and that of 1 layer with 100mm (that is, 0.5 layer) in width. The CFRP sheeting was wrapped spirally over the whole span such that the centerline spacing of sheet width was 197 mm. The confinement ratio imposed by the CFRP sheeting corresponded to that of the CFRP rod in specimens strengthened with a longitudinally prestressed concrete jacket using as an index the shear reinforcement ratio to horizontal section.

The experimental parameters and specimens are detailed in Table 2.

2.3 Loading test procedure

Reversed cyclic loading was applied at two symmetrical points so that the flexural and shear spans were 400 mm and 700 mm, respectively. The overall span was 1,800 mm. Three loading cycles were imposed at (2n-1) times the yield displacement. In some cases, ten loading cycles at each step were carried out so as to investigate seismic behavior. It is known that the load acting at each step in reversed cyclic loading tests falls very little after three loading cycles [4], and a basic loading procedure of three cycles was chosen for this reason. The yield displacement, δ_y, was determined from the change of gradient of each load-displacement curve due to yield of longitudinal reinforcing steel. The yield displacement values were δ_y=7.11 mm for the control specimen and CS specimen. They were δ_y=6.17 mm, 7.06 mm, 8.09 mm, and 7.52 mm for specimens using D13, SBPR930/1080 ϕ11 mm, CFRP tendon, and AFRP tendon, respectively. The ultimate state was defined as the point at which the load dropped below the yield load in the post-peak region.

2.4 Measurements

Displacements at mid-span and at the supports were measured using transducers with a capacity of 100 mm. The mid-span strain of the longitudinal reinforcement D16, SBPR ϕ17 mm for introducing axial force, and tendon were measured using strain gages of length 3 mm, 5 mm, and 5mm, respectively. Moreover, concrete strain as longitudinal prestress and loading were applied was measured using two strain gages of length 60

mm per upper and lower surface of cross-section in mid-span. The amount of longitudinal prestress shown in Table 2 was calculated as the average value of these four strain gauges. The tendon tension as given in Table 2 was measured using a load-cell with a capacity of 200 kN.

3. TEST RESULTS AND DISCUSSION

3.1 Longitudinal prestress

The prestress applied to the jacketing concrete was transmitted to the existing concrete through the bond (joint) between the two. The amount and distribution of prestress in the existing and jacketing concrete, and the bond stress at the joint, were simulated using two-dimensional finite element analysis [5], [6] under the assumption that the joint is perfectly bonded. Discrete elements are used to represent the bonding action at joints.

Assuming that the prestress, which was applied to the jacketing concrete only via a square cut-out plate, was transferred to the existing concrete through the perfect bonding at the joint, the prestress was calculated using the following equation:

$$\sigma_{ps}=E_{cj}\,\varepsilon_{cj}=E_{cj}\,P\,/\,(A_{cj}\,E_{cj}+A_{ce}\,E_{ce}+A_s\,E_s) \tag{1}$$

Where, σ_{ps} is the longitudinal prestress, ε_{cj} is the strain of the jacketing concrete, E_{cj}, E_{ce}, and E_s are the Young's modulus values of the jacketing concrete, existing concrete, and longitudinal reinforcement D16, respectively, and A_{cj}, A_{ce}, and A_s are the net cross-sectional areas of the jacketing concrete, existing concrete, and longitudinal reinforcement D16, respectively.

Quadratic quadrilateral elements with 8 nodes were used for elements of the existing and jacketing concrete. Quadratic truss elements with three nodes were used for the elements representing longitudinal reinforcement D16. Quadratic bond linkage elements [5] with six nodes were used for the bond between longitudinal reinforcement D16 and the existing concrete and for the bond between upper/lower extreme edges of the existing concrete and the jacketing concrete. The bond linkage element owns three nodes in common with concrete element and those with reinforcement/concrete element. Quadratic quadrilateral elements [6] with 16 nodes, consisting of an existing concrete element of 8 nodes and a jacketing concrete element of 8 nodes, were used for the bond of joints in web portion. The width of jacketing concrete element in web portion was 100 mm (=50 mm x 2). Tensile forces on the tendon were treated as distributed loads applied at element nodes at the extreme edge of the beam, so no elements were needed to represent tendons.

The stress-displacement relationship for bond linkage truss elements between upper/lower extreme edges of the existing concrete and for the jacketing concrete can be expressed using the following equation:

$$\sigma=\begin{Bmatrix}\sigma_{\mathrm{n}}\\ \tau_{\mathrm{t}}\end{Bmatrix}=\begin{bmatrix}B_{\mathrm{nn}} & B_{\mathrm{nt}}\\ B_{\mathrm{tn}} & B_{\mathrm{tt}}\end{bmatrix}\begin{Bmatrix}\delta_{\mathrm{n}}\\ \delta_{\mathrm{t}}\end{Bmatrix}=B\cdot\delta \tag{2}$$

Where, σ_n, τ_t are the normal and tangential stresses, respectively, and δ_n, δ_t are the normal and tangential displacements. The coefficient B_{tt} of longitudinal deformation would ideally be determined from experimental data on the characteristics of bonding between concretes, using the same concretes as in this study. However, referring to past experimental data [7] for the bond stress-slip relationship, B_{tt}=3.0 N/mm^3 was adopted in this analysis. On the other hand, B_{nn}=1.0 x 10^4 N/mm^3 and B_{nt}=B_{tn}=0 N/mm^3 were used, because only longitudinal — that is tangential — deformation was considered.

The stress-displacement relationship for bond linkage quadrilateral elements between existing concrete and jacketing concrete can be expressed by the following equation:

$$\sigma=\begin{Bmatrix}\tau_{\mathrm{x}}\\ \tau_{\mathrm{y}}\end{Bmatrix}=\begin{bmatrix}G_{\mathrm{xx}} & 0\\ 0 & G_{\mathrm{yy}}\end{bmatrix}\begin{Bmatrix}\delta_{\mathrm{x}}\\ \delta_{\mathrm{y}}\end{Bmatrix}=G\cdot\delta \tag{3}$$

Where, τ_x, δ_x are tangential stress and displacement in the longitudinal direction of the beam, and τ_y, δ_y are tangential stress and displacement in the depth direction of the beam. Normal deformation in the side concrete elements was ignored. As regards the coefficients in Eq. (3), the same value of G_{xx}=G_{yy}=3.0 N/mm^3 was adopted as for bond linkage truss elements while other coefficients were set at 0 N/mm^3. 3.0mm in

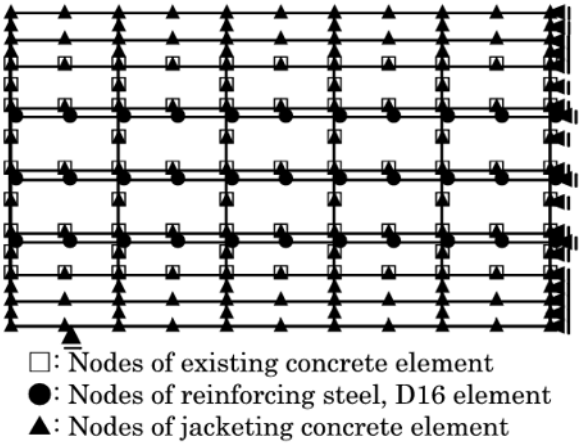

Fig.3 Mesh division

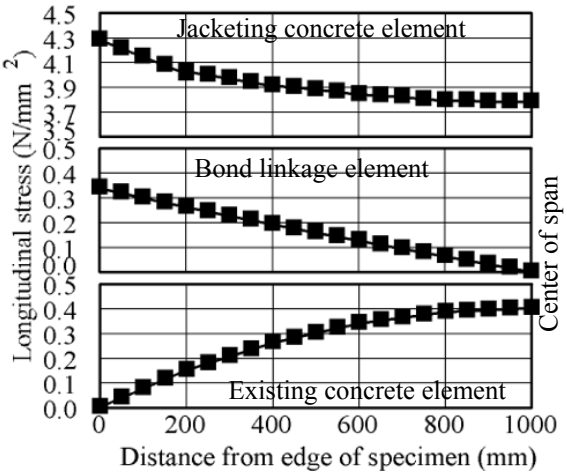

Fig.4 Distributions of longitudinal stress

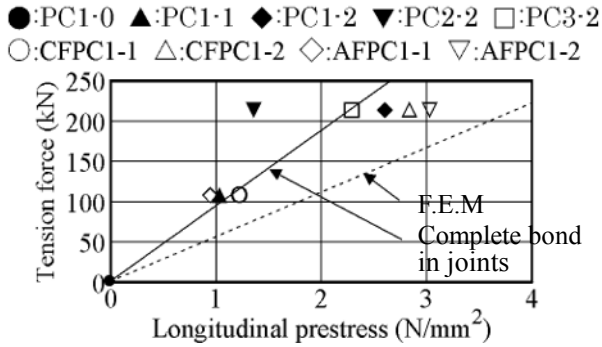

Fig.5 Relationship between tension and longitudinal prestress

thickness, t of bond linkage elements in web portion was used [8].

The compressive strength and Young's modulus of the existing concrete were f'_c=27 N/mm^2 and E_c=2.65 x 10^4 N/mm^2, respectively. Similarly, the compressive strength and Young's modulus of the jacketing concrete were f'_c=45 N/mm^2 and E_c=3.2 x 10^4 N/mm^2, respectively. Poisson's ratio for these concretes was ν=0.1667. The Young's modulus of existing longitudinal reinforcement (D16) was E_s=2.1 x 10^5 N/mm^2. The adopted compressive strength of the existing concrete, f'_c=27 N/mm^2, is less than the experimental value. This value was chosen so as to simulate the longitudinal prestress condition in members consisting of existing concrete of low strength and jacketing concrete of high strength, which is the aim of this analysis. The mesh division for this analysis is shown in Fig. 3. Elastic analysis was conducted by gradually applying longitudinal displacement to each node at the edge of the specimen.

Distributions of stress in jacketing concrete elements, bond linkage quadrilateral elements, and existing concrete elements along the half depth line (150mm) at a total tensile force of 212 kN (=53.0 kN x 4) are shown in Fig. 4. The anchorage zone, meaning the area around the edge of the specimen, had high longitudinal prestress. The longitudinal prestress decreased toward the center of the span. The flexural span had constant longitudinal prestress. Although the sum of longitudinal prestress in the existing and jacketing concrete at every longitudinal position was almost constant, the prestress was higher in the jacketing concrete around the shear span than around the flexural span. This demonstrates that the longitudinal prestress around the shear span in the jacketing concrete effectively controls shear cracking. Bond linkage element stresses decreased linearly with respect to longitudinal length, because the relationship between bond-stress and bond element slippage was assumed to be linear. Furthermore, the longitudinal prestress transmitted to the existing concrete at the center of the span was 10% of that in the jacketing concrete in this analysis, as a result of the assumed bond characteristics.

The relationship between tensile force of the tendon and longitudinal prestress at the center of the span in the jacketing concrete is shown in Fig. 5. The experimental longitudinal prestress increased in proportion to tensile force, except in the case of specimen PC2-2. Thus, longitudinal prestress can be estimated using a linear calculation. Values calculated using Eq. (1) and assuming perfect bonding at joints indicate very good agreement with the experimental values. However, values calculated by FEM analysis are larger than the experimental ones for the same tensile force. It is thought that interactions involving gravel were significant in the experiment, because the surface condition of the existing concrete after treatment with a retarder in the experiment was rougher than that assumed in the analysis. Accordingly, coefficients B_{tt}, G_{xx}, and G_{yy} in the

relationship between bond stress and slippage would in fact have been larger than the assumed values. In other words, if the surface of the existing concrete is roughened sufficiently, longitudinal prestress can be simulated assuming perfect bonding at the joint.

3.2 Failure modes and crack propagation

a) Crack propagation, damage, and failure during loading test

In the case of the control specimen, which had a ratio of shear capacity to flexural capacity of 1.15, although many shear and flexural-shear cracks propagated after yield, compression failure finally occurred during $3\delta_y$ load reversal. Failure was accompanied by crushing of the cover and core concrete due to lack of confinement effect. It was assumed that the control specimen would suffer shear failure under reversed cyclic loading due to loss of shear resistance of the concrete in the shear span. However, the improvement of shear resistance by interaction of aggregates on the surface of shear crack due to axial force led to greater shear capacity and prevented shear failure.

In the case of specimen CS, rupture of the longitudinal CF sheet used for flexural strengthening occurred during $3\delta_y$ load reversal. Later during the same cycle, the lateral CF sheet used for confinement ruptured around the corner of the cross-section in the flexural compression zone. Although CF sheet rupture led to a load reduction, the load did not drop below the yield load. Ultimately, the CS specimen suffered compression failure.

Specimens RC1-0 and RC3-0 suffered ultimate failure during $5\delta_y$ load reversal. Failure occurred when buckling of the longitudinal reinforcing steel in the existing and jacketing concrete resulted in damage to the confinement hooks. This indicates the importance of preventing buckling of the longitudinal reinforcing steel when strengthening structures using a reinforced concrete jacket.

Specimens PC1-0 and PC1-1 suffered compression failure during $7\delta_y$ load reversal. In contrast, specimen PC1-2, which had a ratio of tensile stress to yield strength (P_r) of 0.60, suffered ultimate failure when the tendon ruptured during $7\delta_y$ load reversal. However, the longitudinal reinforcement in the existing concrete prevented any loss in load in these cases. Specimens PC2-2 and PC3-2 suffered compression failure although they had the same ratio of tensile stress to yield strength (P_r) as specimen PC1-2; in these cases, lack of confinement led to serious damage in the flexural compression zone.

In the case of specimen CFPC1-1, significant flexural-shear cracks appeared during $3\delta_y$ load reversal and these ultimately led to shear compression failure. The web in the shear span of the jacketing concrete suffered more serious damage than the existing concrete. This demonstrates that large shear forces acted on the jacketing concrete because of inadequate transmission of shear force between the existing and jacketing concrete [9]. It is assumed that difficulty in wetting of the existing concrete surface during casting of the jacketing led to drying, so bonding at the joint was insufficient. This can be inferred because shear failure occurred at the bottom of the shear span where the jacketing concrete was cast. Furthermore, the angle of the shear reinforcement in the case of spiral CFRP was not effective to oppose the principal tensile stress in the shear span. Specimen CFPC1-2 suffered ultimate failure as a result of tendon rupture during $5\delta_y$ load reversal. However, the longitudinal reinforcement in the existing concrete prevented any loss in load.

Specimen AFPC1-1 suffered compression failure during $7\delta_y$ load reversal. Specimen AFPC1-2 suffered ultimate failure as a result of tendon rupture during $5\delta_y$ load reversal. However, in

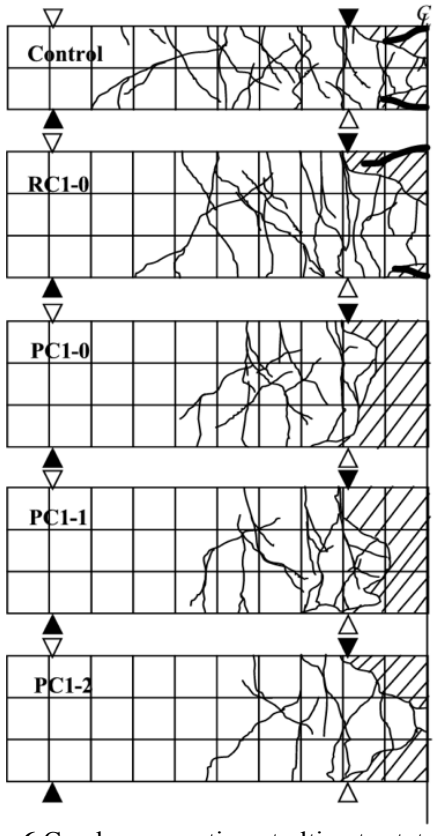

Fig.6 Crack propagation at ultimate state

both cases, the longitudinal reinforcement in the existing concrete prevented any loss in load.

b) Crack propagation at the ultimate state

Figure 6 shows crack propagation at the ultimate state. In the control specimen, many shear and flexural-shear cracks were apparent. Specimen RC1-0 had flexural cracks with a wide distribution. On the other hand, specimen PC1-2, which was strengthened using a longitudinally prestressed concrete jacket, had fewer shear cracks and these were limited to the region around the flexural span. This result may lead to a simple method of repair and quick restoration to serviceability after an earthquake. Moreover, the crack propagations for specimens PC1-0, PC1-1, and PC1-2 show that the number of small cracks in the shear span fell somewhat as longitudinal prestress was increased. It was also observed that longitudinal prestress improved the closing of cracks during loading tests. However, the influence of longitudinal prestress on shear crack angle to the neutral axis in the shear span is not very clear. Thus these observations indicate that effective control of cracking can be achieved by introducing longitudinal prestress. Such control of cracking by introducing longitudinal prestress is effective for improving durability and good appearance after the earthquake.

3.3 Load-displacement curves

Load-displacement curves are shown in Fig. 7 along with derived curves obtained by sectional moment-curvature analysis (assuming the plane-sections hypothesis). In this analysis, stress-strain models for confined concrete using CF sheet [10], steel confinement [11], and CFRP or AFRP confinement [12] were used to simulate the core concrete, including the existing concrete. A JSCE model [13] was used for the reinforcing steel or steel tendon, and a JSCE model [14] was also used for the CFRP or AFRP tendons. Strength and Young's modulus values for each element were those obtained by material tests. Furthermore, perfect bonding between existing concrete and the jacketing concrete was assumed; that is, members strengthened

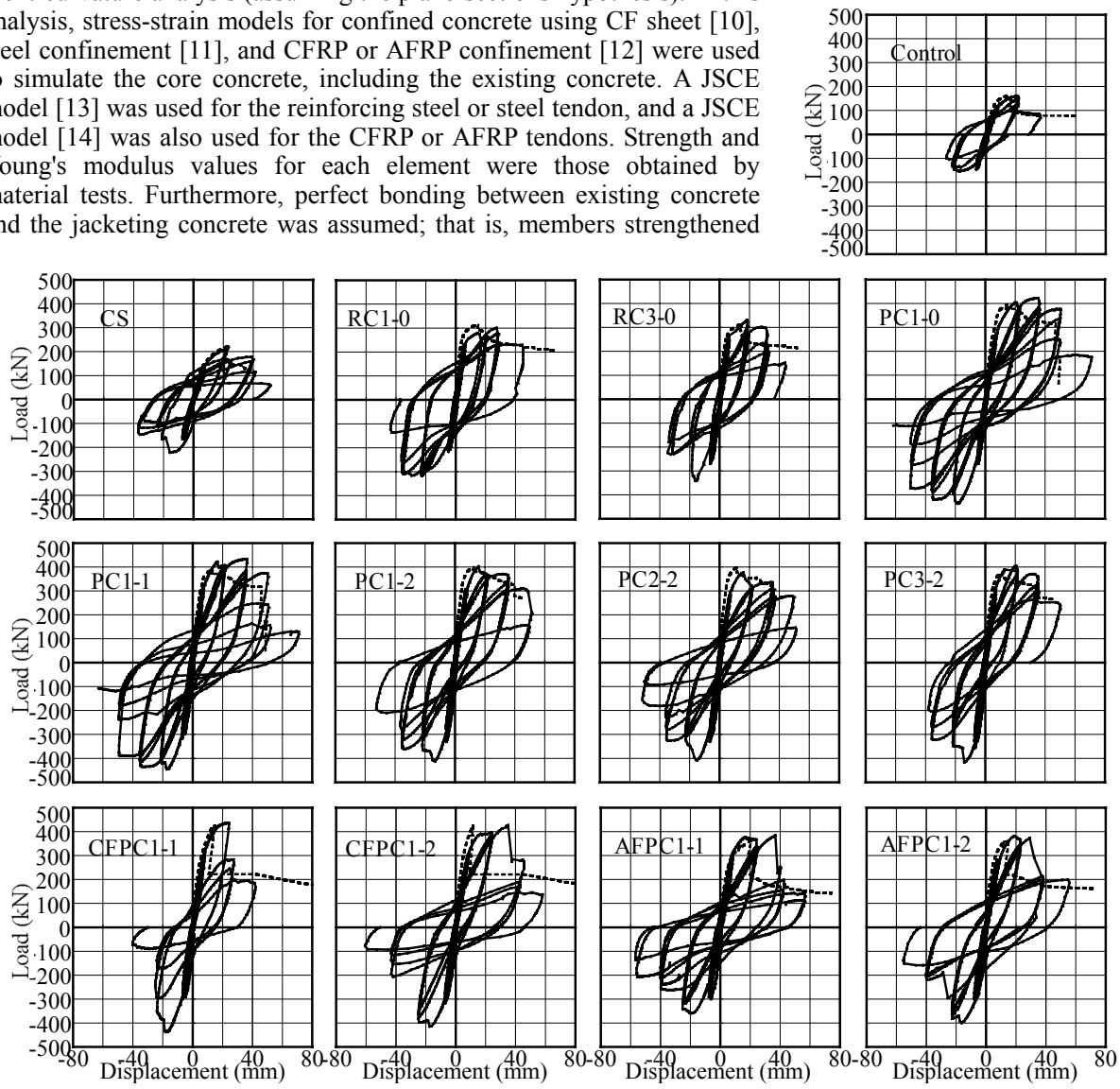

Fig.7 Load-displacement curves ____ Exp. ..... Cal.

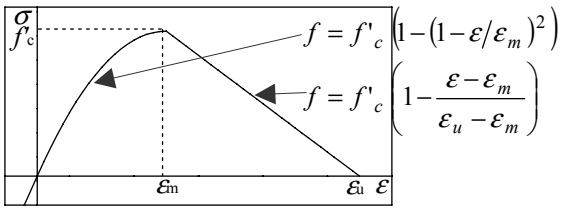

Fig.8 Stress-strain relationship of concrete

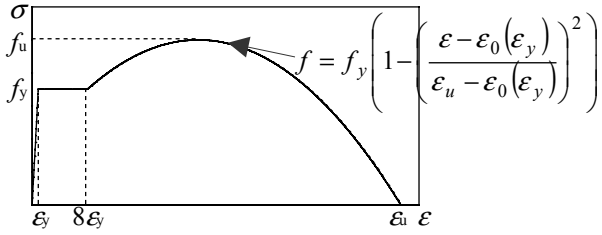

Fig.9 Stress-strain relationship of reinforcing steel

with reinforced concrete and longitudinally prestressed concrete were assumed to be monolithic structures in which only the mechanical properties of the jacketing concrete differed from those of the existing concrete.

The experimental load-displacement curves of members strengthened with longitudinally prestressed concrete are somewhat spindle-shaped, because the existing portion is a reinforced concrete member. Curves for specimens PC1-2, CFPC1-2, and AFPC1-2 no loss of load occurred because of the presence of reinforcing steel in the existing concrete, although they suffered tendon rupture.

A comparison of the calculated curves with the experimental ones indicates quite good agreement from the viewpoint of yield or maximum load, despite the assumption of a monolithic structure. This means that, if the surface on the existing concrete is sufficiently roughened as in this experiment, members strengthened with longitudinally prestressed concrete can be designed on the assumption that perfect bonding is achieved at the joint. The failure of specimen PC1-2, which had the largest ultimate strain in the upper extreme fiber among specimens PC1-2, PC2-2, and PC3-2, was by tendon rupture and this corresponds to the experimental result. Also, the calculated results for specimens with tensile forces of 0 kN and 26.5 kN show ultimate failure by tendon rupture, although only the specimen with a volumetric confinement ratio of 0.92% and tensile force of 53.0 kN suffered tendon rupture in the experiment.

These calculated curves were derived from a simulation of one-directional monotonous loading. On the other hand, great damage occurred in the flexural compression zone in the experiment after three loading cycles. Thus, the strain in the tendon did not reach the ultimate strain in the case of an initially small tensile force.

Next, in order to investigate the influence of joint bonding on the flexural behavior of members strengthened with a reinforced concrete jacket, two-dimensional finite element analysis using discrete elements similar to that in 3.1 was implemented. In this analysis, in addition to the elements used in 3.1, quadratic beam elements with thee nodes, and taking flexural rigidity EI into account were used for the longitudinal reinforcement in the existing concrete. Quadratic truss elements with three nodes were used for the longitudinal reinforcement in the jacketing concrete. Linear truss elements, in which bonding between reinforcement and concrete is ignored, were used for shear reinforcement in the jacketing concrete.

The relationship between longitudinal stress and strain for the existing and jacketing concrete is shown in Fig. 8. The concrete elements were assumed to be anisotropic, with the relationship being nonlinear in the longitudinal direction but constant vertically. The concrete elements did not have a tension softening zone. Consequently, quadrilateral crack elements [15] were adopted to model the flexural cracks between concrete elements at positions 600 mm, 800 mm, and 1,000 mm from the edge of specimen, in order to prevent the buildup of excessive tensile stress in concrete elements. These crack elements consist of two concrete elements of three nodes each just like the bond linkage elements. These crack elements were assumed to transmit only the normal stress.

The relationship between stress and strain for the longitudinal reinforcement in the existing and jacketing concrete is shown in Fig. 9. Although a stress-strain model that unifies the relationship from the strain hardening zone until rupture was used to stabilize convergence, strains in the longitudinal reinforcement elements were only those up to the limit of the strain hardening zone in this analysis. Accordingly, the zone in which stress falls in this model does not influence the calculated result. In addition to the bond stress-slip relationships of 3.1 for bond linkage elements at joints, the relationship in which nodes of jacketing concrete element were fixed in those of existing concrete element (where no slip displacement occurred) was adopted assuming complete bond in joints. Furthermore, $B_{tt}=G_{xx}=G_{yy}=1.0 \times 10^{-10}$ N/mm^3 was adopted as the coeffi-

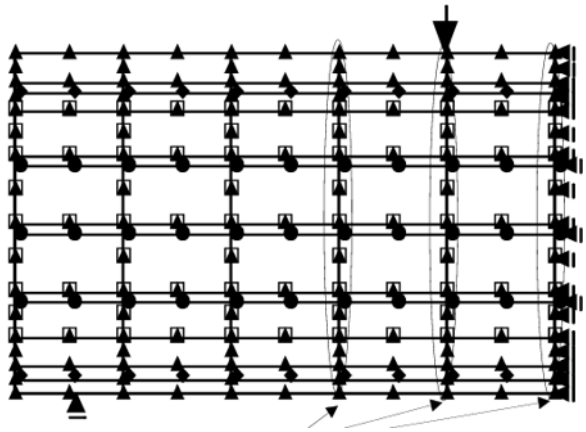

□ : Nodes of existing concrete element
● : Nodes of reinforcing steel, D16 element
▲ : Nodes of jacketing concrete element
◆ : Nodes of reinforcing steel element in jacketing concrete

Fig.10 Mesh division

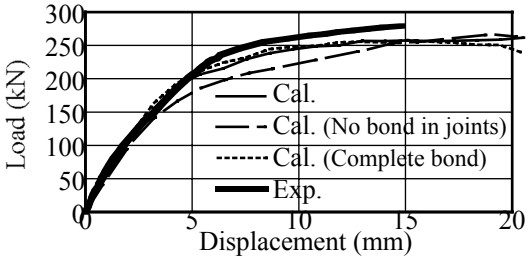

Fig.11 Load-displacement curves

▲:Control ▼:RC1-0 ●:PC1-0 ■:PC1-1 ◆:PC1-2
White symbols: calculated values for each specimen

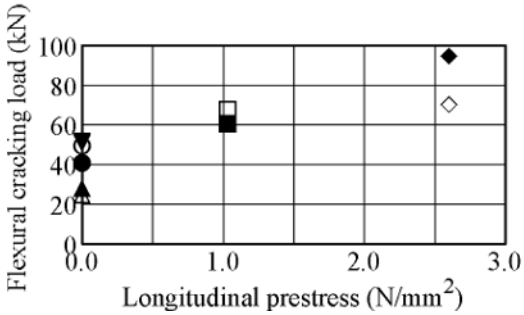

Fig.12 Flexural cracking load

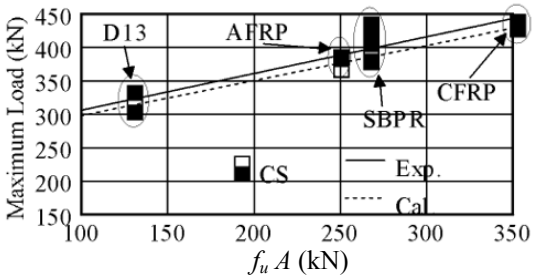

Fig.13 Maximum load

cient in the bond stress-slip relationships, assuming no bonding at joints. The relationship between these bond linkage elements was then linear.

Nonlinear analysis was carried out using the mesh division shown in Fig. 10. Increasing vertical displacement was applied at the upper node at a point 800 mm from the edge of the specimen.

The analytical load-displacement curves for specimen RC1-0, which has 4-D13 as the longitudinal reinforcement, are shown in Fig.11 along with the experimental results. The calculated curves assuming perfect bonding at joints indicate the highest stiffness, and this corresponds well with the experimental findings. Therefore, it is assumed that perfect bonding is achieved by treating the surface layer of the existing concrete as in this experiment. However, the calculated curve using the coefficient $B_{tt}=G_{xx}=G_{yy}=3.0$ N/mm^3 yielded almost the same stiffness as the one assuming perfect bonding. Although the bond stress-slip relationship in bond linkage elements was taken to be linear, the characteristics of bonding at joints needs to be investigate further.

3.4 Flexural cracking load

The influence of longitudinal prestress on flexural cracking load is shown in Fig. 12 along with calculated values. The calculated results were obtained by the moment-curvature analysis described in 3.3. The experimental and calculated flexural cracking loads increase linearly as the longitudinal prestress rises. Accordingly, longitudinal prestress can control flexural cracking. Furthermore, flexural members are easier to repair after an earthquake.

3.5 Maximum load

The influence of different types of longitudinal reinforcement on maximum load is shown in Fig. 13 along with calculated values obtained by moment-curvature analysis. The maximum load increased for all strengthened specimens, and the increase was linear with respect to (tensile strength, f_u) x (cross-sectional

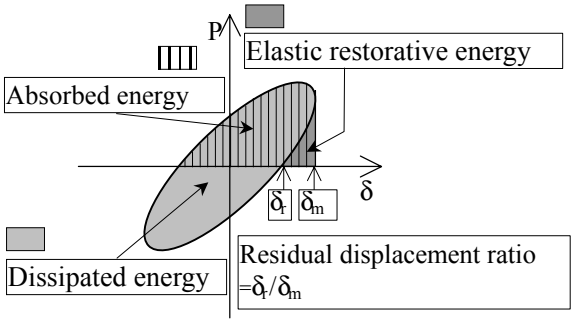

Fig.14 Definition of absorbed, dissipated and elastic restorative energy, and residual displacement ratio

area of reinforcement, A). A comparison of calculated maximum loads with experimental values indicates good agreement. Moreover, the maximum load in the case of specimens CFPC1-1 and CFPC1-2 was larger than that of specimen CS, which had the same quantity of carbon fiber as the specimens CFPC1-1 and CFPC1-2. The greater cross-sectional area of the flexural compression zone as a result of the concrete jacket is the cause of this higher maximum load.

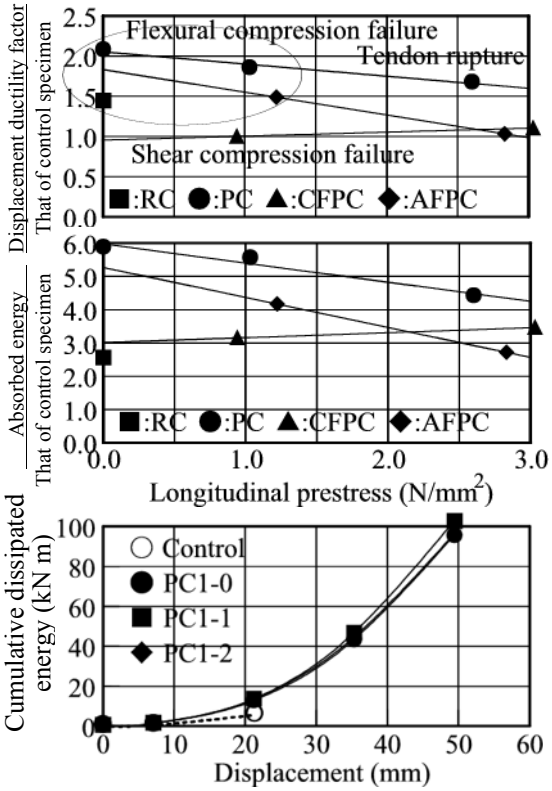

Fig.15 Influence of longitudinal prestress on ductility

3.6 Ductility

The displacement ductility factor ($\mu=\delta_u/\delta_y$), absorbed energy, and dissipated energy [16] were adopted as indices of ductility. The absorbed and dissipated energy are shown in Fig. 14, along with residual displacement ratio and elastic restorative energy as discussed in 3.7. Both areas, that enclosed by the x-axis and the load-displacement envelope and that enclosed by the hysteresis loop, represent energy capacity. However, the absorbed and dissipated energy were investigated separately because the dimensions of elastic restorative energy change the ratio of dissipated energy to absorbed energy.

a) Influence of longitudinal prestress on ductility

The influence of longitudinal prestress on displacement ductility factor, absorbed energy, and accumulated dissipated energy up to ultimate state are shown in Fig. 15. The displacement ductility factors and absorbed energy of strengthened specimens were larger than those of the control specimen. The difference in absorbed energy between strengthened specimens and the control specimen was greater than the difference in displacement ductility factor. Although displacement ductility factor did not increase dramatically as a result of the rise in yield displacement caused by using a reinforcing concrete jacket for strengthening, the use of high tensile strength tendons did achieve an increase in flexural capacity and so more energy was absorbed or dissipated. This means that strengthening using a longitudinally prestressed concrete jacket is effective not only for increasing the flexural capacity but also for improving energy ductility.

In all strengthened specimens with the exception of CFPC1-1, which suffered shear compression failure, the displacement ductility factor and absorbed energy decreased as longitudinal prestress increased. This is because a large load reduction resulted from damage in the flexural compression zone and rupture of the tendon under large longitudinal prestress. On the other hand, the influence of longitudinal prestress on dissipated energy was less than that on displacement ductility factor and absorbed energy. This means that, although the elastic restorative energy and absorbed energy were reduced more significantly by the lower load (which resulted from damage in the flexural compression zone) as longitudinal prestress increased, the area of the hysteresis loop did not change.

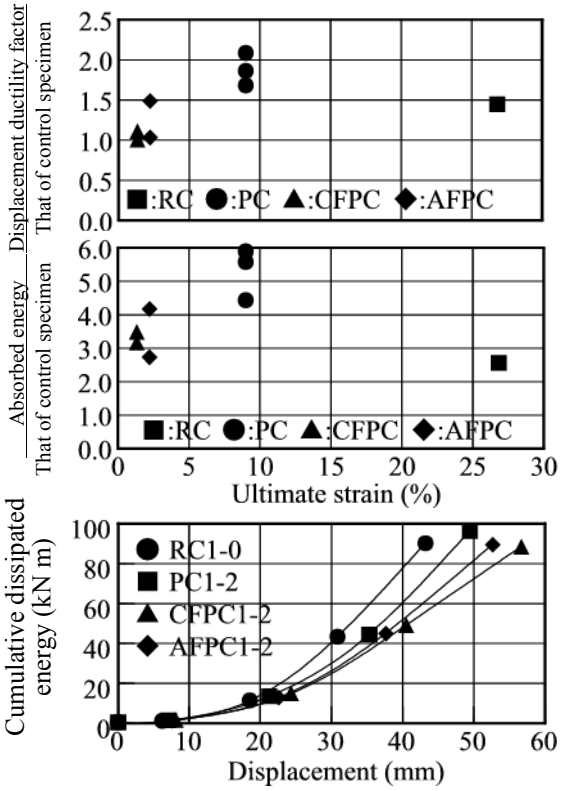

Fig.16 Influence of ultimate strain of longitudinal reinforcement on ductility

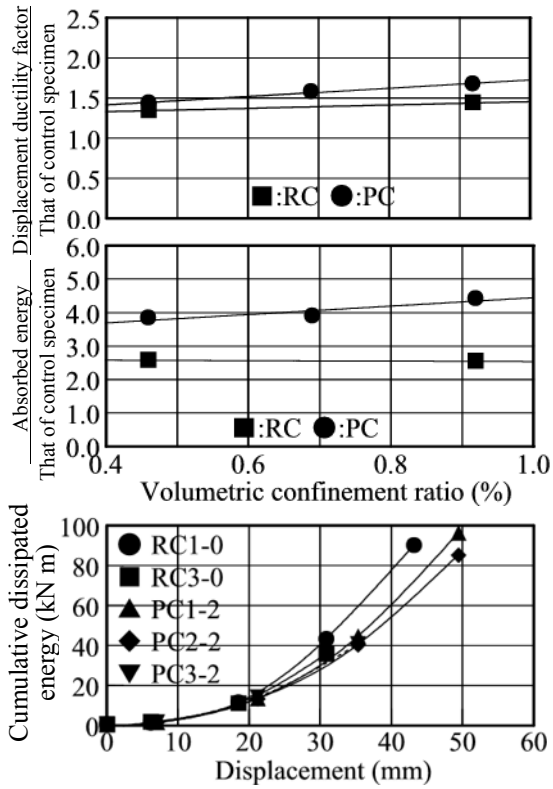

Fig.17 Influence of volumetric confinement ratio on ductility

b) Influence of ultimate longitudinal reinforcement strain on ductility

The influence of the ultimate strain of the longitudinal reinforcement in the jacketing concrete on displacement ductility factor, absorbed energy, and accumulated dissipated energy up to ultimate state are shown in Fig. 16. The displacement ductility factor and absorbed energy of specimens with SBPR tendons were greater than those of specimens with FRP tendon, regardless of failure mode. Specimen RC1-0 is an exception to this; here, ductility did not increase sufficiently as a result of damage to the confinement hooks. Firstly, the rupture of FRP tendons occurred earlier than the rupture of SBPR tendons, because ultimate strain of FRP tendons was smaller than that of SBPR tendons. Secondly, the load reduction resulting from damage to the flexural compression zone was larger in the case of SBPR, because the high elasticity of FRP tendon, and especially CFRP tendons, led to much higher flexural compression stress after yielding of the strengthened member. For these reasons, the displacement ductility factor and absorbed energy of specimens using SBPR tendons were greater than for FRP tendons. On the other hand, although the maximum load and absorbed energy of specimens strengthened with longitudinally prestressed concrete using high-strength tendons were greater than in the case of RC specimens, the accumulated dissipated energy of the RC specimens was the highest. This is because the RC specimens had little elastic restorative energy and spindle-shaped hysteresis loops. Furthermore, the rate of increase in accumulated dissipated energy of specimens with FRP tendons having elastic properties, and especially the CFRP tendon, was small after $3\delta_y$ due to damage in the flexural compression zone.

c) Influence of volumetric confinement ratio on ductility

The influence of volumetric confinement ratio of the jacketing concrete on displacement ductility factor, absorbed energy, and accumulated dissipated energy up to ultimate state is shown in Fig. 17. In the case of specimens strengthened with a longitudinally prestressed concrete jacket, the displacement ductility factor, absorbed energy, and accumulated dissipated energy did not increase much as the volumetric confinement ratio increased, because the specimen with a volumetric confinement ratio of 0.92% suffered rupture of the tendon. The RC specimens suffered ultimate failure during $5\delta_y$ load reversal, because the longitudinal reinforcing steel in the existing and jacketing concrete suffered damage to the confinement hooks. Accordingly, the influence of volumetric confinement ratio on the ductility of the RC specimens was not notable, and RC

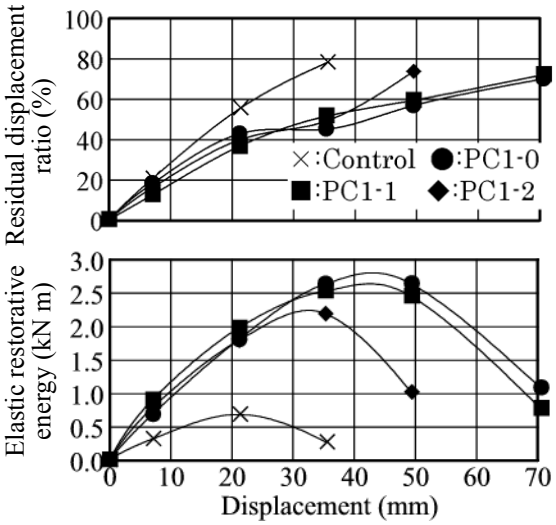

Fig.18 Influence of longitudinal prestress on elastic restoration

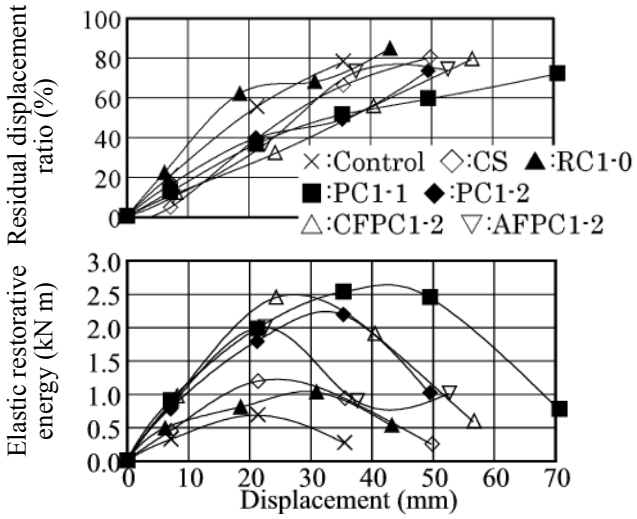

Fig.19 Influence of longitudinal reinforcement on elastic restoration

specimens were not superior to PC specimens from the point of view of displacement ductility factor. The difference in absorbed energy between RC specimens and PC specimens was larger than the difference in displacement ductility factor. This is because the maximum load and absorbed energy of PC specimens using tendons with high strength were high.

3.7 Elastic restoration behavior

The residual displacement ratio and elastic restorative energy (in Fig. 14) during the first loading cycle at $(2n-1)\delta_y$ were used as indices of elastic restoration.

a) Influence of longitudinal prestress on elastic restoration behavior
The influence of longitudinal prestress on residual displacement ratio and elastic restorative energy is shown in Fig. 18. PC specimens had lower residual displacement ratios and larger elastic restorative energies than RC specimens at the same loading displacement. However, when specimen PC1-2, which had the highest longitudinal prestress, suffered tendon rupture at the $7\delta_y$ load reversal, the residual displacement ratio increased and the elastic restorative energy decreased significantly. Therefore, the load reduction accompanying tendon rupture dramatically affects the elastic restoration behavior of a member strengthened with a longitudinally prestressed concrete jacket.

b) Influence of different longitudinal reinforcement on elastic restoration behavior
The influence of various types of longitudinal reinforcement in the jacketing concrete on residual displacement ratio and elastic restorative energy is shown in Fig. 19. Specimens with CFRP tendons low residual displacement ratios and large elastic restorative energies around $3\delta_y$. On the other hand, specimens with SBPR tendons had small residual displacement ratios and large elastic restorative energies after $3\delta_y$. This demonstrates that strengthening a member with a longitudinally prestressed concrete jacket using a tendon with good elastic properties, such as a CFRP tendon, yields improved elastic restoration capacity. However, in order to maintain this good elastic restoration in the post-peak region, it is essential to prevent rapid load loss due to damage in the flexural compression zone and tendon rupture. This can be achieved by choosing a tendon with some plastic deformability.

c) Influence of volumetric confinement ratio on elastic restoration behavior
The influence of volumetric confinement ratio of the jacketing concrete on residual displacement ratio and elastic restorative energy is shown in Fig. 20. In RC specimens, which suffered ultimate failure due to damage of the confinement hooks during $5\delta_y$ load reversal, the Influence of volumetric confinement ratio on elastic restoration is not significant. Specimens PC2-2 and PC3-2, which suffered flexural compression failure, had smaller residual displacement ratios and larger elastic restorative energies than specimen PC1-2,

which suffered tendon rupture. A high volumetric confinement ratio increases the ultimate strain in the upper extreme fiber in the flexural compression zone. Accordingly, a rapid load loss due to damage in the flexural compression zone can be prevented. However, it is assumed that a high volumetric confinement ratio will alter the failure mode of members strengthened with a longitudinally prestressed concrete jacket containing a tendon, since the ultimate strain is less than for normal reinforcement; that is, the failure mode will change from flexural compression failure to tendon rupture. Therefore, in order to maintain good elastic restoration in the post-peak region, the volumetric confinement ratio should be determined such that the strengthened member ultimately fails in flexural compression.

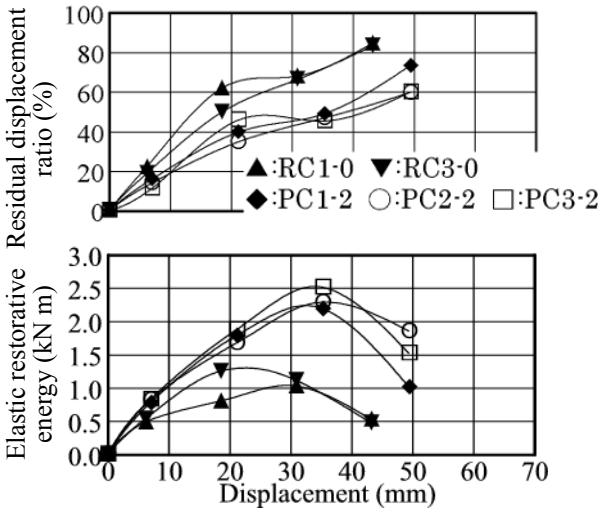

Fig.20 Influence of volumetric confinement ratio on elastic restoration

4. CONCLUSIONS

In this study, the flexural behavior of RC members strengthened with a longitudinally prestressed concrete jacket was investigated under reversed cyclic loading. This jacket strengthening method improves elastic restoration, while also increasing flexural capacity and ductility. The aim is to achieve simple repairs, quick restoration to serviceability, durability, and good appearance after an earthquake.

The conclusions obtained in this study are as follows:

(1) Longitudinal prestress can be estimated through linear calculation assuming perfect bonding between existing and jacketing concrete. The distribution of longitudinal prestress in existing and jacketing concrete, and the bond stress, can be simulated by two-dimensional finite element analysis using discrete elements representing the bond between existing and jacketing concrete.

(2) Members strengthened with a longitudinally prestressed concrete jacket had fewer shear cracks and the cracks that did form were limited to the area around the flexural span. Furthermore, the flexural cracking load rose as the longitudinal prestress increased. Such control of cracking by introducing longitudinal prestress is effective for improving durability and good appearance after the earthquake.

(3) The yield and maximum capacity of members strengthened with a longitudinally prestressed concrete jacket are greater than for members strengthened with a reinforced concrete jacket with the same longitudinal reinforcement ratio. This is because a high-tensile strength tendon is used for the longitudinal reinforcement. The yield and maximum capacity can be estimated by assuming the plane-sections hypothesis and perfect bonding between existing and jacketing concrete.

(4) Members strengthened with longitudinally prestressed concrete exhibit improved energy absorption as well as flexural capacity. The ductility of members strengthened using SBPR tendons is better than for those using FRP tendons.

(5) Members strengthened with longitudinally prestressed concrete in which a tendon with good elastic properties is used offer improved elastic restoration. Furthermore, elastic restoration can be maintained into the post-peak region if a tendon with some plastic deformation is chosen and if the confinement of the jacketing concrete is kept within an appropriate upper limit.

ACKNOWLEDGMENTS

The authors wish to acknowledge Dr. T. Kojima, Professor of Ritsumeikan Univ. and Mr. K. Hibino, a doctoral student at Ritsumeikan Univ., for their valuable contributions to this study.

REFERENCES

[1] JCI Kinki branch, Technical Committee Report, May. 1999.
[2] JSCE, Standard Specification for Design of Concrete Structures, Mar. 1996.
[3] JSCE, Standard Specification for Design of Concrete Structures, Sep. 1991, pp.165-166.
[4] Machida, A., Present Stage of Studies on Earthquake Resistant Design of Reinforced Concrete Structures, Journal of Materials, Concrete Structures and Pavements, JSCE, No.366/V-4, Feb. 1986, pp1-11.
[5] Kojima, T., Takagi, N., and Hibino, K., Development of a Discrete Bond Linkage Element Between Concrete and Reinforcing Bar, Second International Conference on Engineering Materials, Vol.1, Aug. 2001, pp.315-326.
[6] Hibino, K., Nakagoshi, T., Kojima, T., and Takagi, N., FEM Analysis of Dynamic Response of Seismic Strengthened RC Pier, Proc. of the 54th Annual Conference of the JSCE, V-287, Sep. 1999. pp.574-575.
[7] Makitani, T., Katori, K., and Hayashi, S., An Evaluation of Surface Roughness of Pre-Cast Concrete Panel and Experiments on Ability of Shear Transfer through Construction Joint, Proc. of the Japan Concrete Institute, Vol.17, No.2, Jul. 1995. pp.171-176.
[8] Nippon Jikkou Co. Ltd, Technical data on retarder
[9] Yamamoto, T., Hattori, A., and Miyagawa, T., Application of Fiber Reinforced Plastic Rod to Strengthening with Prestressed Concrete Jacket, Proc. of the 53th Annual Conference of the JSCE, V-438, Oct. 1998. pp.876-877.
[10] Hosotani, M., Kawashima, K., and Hohsikuma, J., A Stress-Strain Model for Concrete Cylinders Confined by Carbon Fiber Sheets, Journal of Materials, Concrete Structures and Pavements, JSCE, No.592/V-39, May. 1998, pp37-52.
[11] Fujii, M., Kobayashi, K., Miyagawa, T., Inoue, S., and Matsumoto, T., Investigation on Application of Stress-Strain Relationship of Laterally Confined Concrete, Review of the 42nd General Meeting, Cement Association of Japan, 1988, pp.246-249.
[12] Mutsuyoshi, H., Taniguchi, H., Kita, T., and Machida, A., Improvement in ductility of PC members reinforced with FRP, Journal of Materials, Concrete Structures and Pavements, JSCE, No.460/V-18, Feb. 1993, pp103-111.
[13] JSCE, Standard Specification for Design of Concrete Structures, Mar. 1996, pp.36-37.
[14] JSCE, Recommendations for Design and Construction of Concrete Structures Using Continuous Fiber Reinforcing Materials (Construction), Concrete Library 88, Sep. 1996, pp.10.
[15] JCI Kinki branch, Technical Committee Report, May. 1999, pp.322-330.
[16] Chung, S. Y., Meyer, C., and Shinozuka, M., Modeling of Concrete Damage, ACI Structural Journal, Vol.86, No.3, May-June. 1989.